

A Combined Approach Towards Consistent Reconstructions of Indoor Spaces based on 6D RGB-D Odometry and KinectFusion

Nadia Figueroa, Ecole Polytechnique Federale de Lausanne (EPFL)

Haiwei Dong, University of Ottawa

Abdulmotaleb El Saddik, University of Ottawa and New York University AD

We propose a 6D RGB-D odometry approach that finds the relative camera pose between consecutive RGB-D frames by keypoint extraction and feature matching both on the RGB and depth image planes. Furthermore, we feed the estimated pose to the highly accurate KinectFusion algorithm, which uses a fast ICP (Iterative-Closest-Point) to fine-tune the frame-to-frame relative pose and fuse the Depth data into a global implicit surface. We evaluate our method on a publicly available RGB-D SLAM benchmark dataset by Sturm et al. The experimental results show that our proposed reconstruction method solely based on visual odometry and KinectFusion outperforms the state-of-the-art RGB-D SLAM system accuracy. Moreover, our algorithm outputs a ready-to-use polygon mesh (highly suitable for creating 3D virtual worlds) without any post-processing steps.

General Terms: 3D Mapping, RGB-D Sensing, Visual Odometry

Additional Key Words and Phrases: Indoor Mapping, Kinect, Benchmark Datasets, Evaluation

ACM Reference Format:

Nadia Figueroa, Haiwei Dong and Abdulmotaleb El Saddik. 2013. A Combined Approach Towards Consistent Reconstructions of Indoor Spaces based on 6D RGB-D Odometry and KinectFusion. *ACM Trans. Intell. Syst. Technol.* V, N, Article A (January YYYY), 10 pages.

DOI: <http://dx.doi.org/10.1145/0000000.0000000>

1. INTRODUCTION

In this work, we aim at generating consistent reconstructions of indoor spaces using a freely moving hand held RGB-D sensor, that can lead to the analysis and interpretation of the 3D reconstructed indoor models by automatically generating smart representations, such as 3D CAD models (consequently 3D printed models) and 2D layouts. With the release of low-cost RGB-D sensors such as the Microsoft Kinect¹ and the PrimeSense 3D Sensor², the possibility of reconstructing our surroundings, objects and even ourselves in 3D has been reached. Thus, we present an algorithm that is targeted at using these devices.

We propose a novel VO (Virtual Odometry) algorithm based on the RGB-D data of consecutive frames and *KinFu Large Scale*, which shows promising results compared

¹Microsoft Kinect. <http://www.xbox.com/en-us/kinect>

²Primesense 3D Sensor. <http://www.primesense.com/>

Author's addresses: N. Figueroa is with the Learning Algorithms and Systems Laboratory, Ecole Polytechnique Federale de Lausanne (EPFL), Switzerland; H. Dong is with the School of Electrical Engineering and Computer Science, University of Ottawa, Ontario, Canada; A. El Saddik is with the School of Electrical Engineering and Computer Science, University of Ottawa and is visiting the Division of Engineering, New York University Abu Dhabi.

Permission to make digital or hard copies of part or all of this work for personal or classroom use is granted without fee provided that copies are not made or distributed for profit or commercial advantage and that copies show this notice on the first page or initial screen of a display along with the full citation. Copyrights for components of this work owned by others than ACM must be honored. Abstracting with credit is permitted. To copy otherwise, to republish, to post on servers, to redistribute to lists, or to use any component of this work in other works requires prior specific permission and/or a fee. Permissions may be requested from Publications Dept., ACM, Inc., 2 Penn Plaza, Suite 701, New York, NY 10121-0701 USA, fax +1 (212) 869-0481, or permissions@acm.org.

© YYYY ACM 2157-6904/YYYY/01-ARTA \$15.00

DOI: <http://dx.doi.org/10.1145/0000000.0000000>

to a state-of-the-art RGB-D SLAM system. In contrast to the experiments presented by [Whelan et al. 2012], our approach combines VO and ICP (Iterative-Closest-Point) as coarse-to-fine alignment method, i.e. VO provides a coarse alignment (rough rigid motion guess) between the consecutive camera poses and ICP fine-tunes (or corrects) this initial estimate. This procedure has been shown to generate consistent reconstructions from RGB-D data [Figueroa et al. 2012], as opposed to using switching strategies between different estimation approaches which might ignore good quality alignments due to the user-set threshold.

Our indoor 3D reconstruction algorithm is an iterative two-step procedure based on an adaptation of KinectFusion algorithm [Newcombe et al. 2011] to a novel 6D RGB-D odometry. We propose a robust 6D RGB-D odometry algorithm which considers useful information from both RGB and Depth images to estimate the 6D rigid motion of a moving RGB-D Sensor. The result of the estimated odometry is used as an initial transformation guess to the KinectFusion’s fast ICP algorithm. As the original KinectFusion relies solely the ICP algorithm based on depth data, it is prone to camera pose estimation failures in the presence of planar surfaces with undescriptive 3D features. Thus, we present two contributions in this paper: (i) the novel 6D RGB-D odometry algorithm and (ii) an improvement to the KinectFusion algorithm by combining it with our proposed odometry estimation. Furthermore, we evaluate our proposed approach on a publicly available RGB-D benchmark dataset used for the evaluation of RGB-D SLAM systems [Sturm et al. 2012] and compare it with the publicly available results of the RGB-D SLAM presented by [Endres et al. 2012].

This paper is organized as follows. In Section 2, we present the problem formulation of the targeted application in this work and in Section 3 we describe the proposed approach and present a detailed description of each component. In Section 4, we provide the evaluation results of our system applied on the RGB-D benchmark and present promising results. Finally, we conclude the whole paper in Section 5.

2. PROBLEM FORMULATION

The indoor mapping problem using a freely moving handheld sensing device is based on estimating the pose of the sensor (i.e. camera pose C) for each k -th frame from a recorded trajectory of the sensing device and simultaneously building a map of the environment with the estimated camera poses and acquired 3D representations of each frame. The 6DOF camera pose $C_k = (R_k, t_k)$ is a rigid body transformation matrix, where $R_k \in \mathbb{SO}_3$, $t_k \in \mathbb{R}^3$ and k is the k -th camera pose for $k = 1, \dots, N$ (N =total number of frames/poses). In order to generate the trajectory of successive camera poses, we need to estimate the rigid motion between consecutive camera poses $C_{k-1} \rightarrow C_k$. This can be defined with a homogenous transformation $T_{k-1}^k = (R_{k-1}^k, t_{k-1}^k)$ of a camera pose C_{k-1} with respect to camera pose C_k as $C_k = T_{k-1}^k(C_{k-1})$.

By setting the initial camera pose C_0 to an identity matrix or a specified initial pose, any successive camera pose can be estimated by incrementally multiplying the rigid motion transformations between consecutive frames, thus C_k can be re-written as

$$C_k = \prod_{i=1}^k T_{i-1}^i C_0 = T_{k-1}^k \left(\prod_{i=1}^{k-1} T_{i-1}^i C_0 \right). \quad (1)$$

It can be inferred by Equation 1 that if any estimated T_{i-1}^i are erroneous or present drift, these errors are carried out throughout the complete trajectory. This error can be reduced and evenly distributed throughout the trajectory by identifying loop closures and optimizing the pose trajectories as in SLAM approaches. However, in this paper we propose an approach that estimates the incremental rigid motion T_{i-1}^i with high

accuracy using both RGB and Depth information in the pose estimation method and reaches the same accuracy as a SLAM-based approach. In the following section, we describe in detail our proposed approach.

3. OUR PROPOSED INDOOR MAPPING ALGORITHM

In order to obtain the best estimate of the incremental rigid motions T_{k-1}^k between consecutive frames $C_{k-1} \rightarrow C_k$ we propose a two-step coarse-to-fine pose estimation approach. Initially, we introduce a novel visual odometry algorithm based on the RGB-D data of consecutive frames, which is thoroughly described in Section 3.1. This resulting estimated pose from our VO is used as a coarse estimation, i.e. an initial guess to a fine estimation method (fast-ICP) used within the KinectFusion algorithm introduced by [Newcombe et al. 2011] (described in Section 3.2).

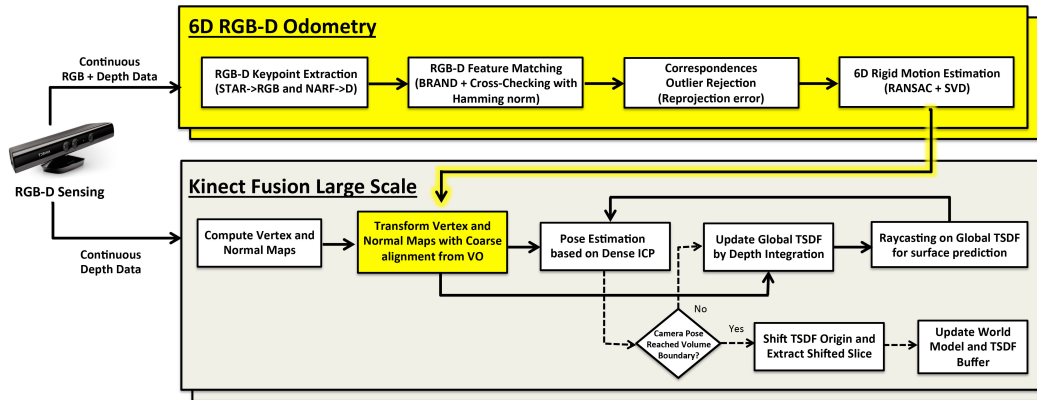


Fig. 1: Schematic overview of our approach.

The map is then incrementally updated in a global implicit model of the surface inferred from the aligned depth data and as the trajectory finalizes the model can be obtained as a 3D volumetric representation or a polygon mesh by applying the marching cubes algorithm on the 3D data. These steps are illustrated in a schematic overview of our approach in Fig. 1. The yellow blocks and yellow shadowed arrows represent our contributions. The dashed lines represent the KinectFusion extension for large scale environments implemented by Heredia and Favier³.

3.1. 6D RGB-D Odometry

Visual odometry (VO) is the process of estimating the incremental pose of a visual sensing device, either standalone or mounted on an agent (i.e. robot, human or vehicle), by using the captured images [Scaramuzza and Fraundorfer 2011]. The standard VO approach is based on the following components: (i) feature detection, (ii) feature matching/tracking and (iii) outlier removal (generally based on RANSAC). In the past years, RGB images have been used to extract visual appearance information from the scenes with the well-known Scale Invariant Feature Transform (SIFT) [Lowe 2004] and Speed Up Robust Features (SURF) [Bay et al. 2008] algorithms. However, when applying them on real world environments, several issues arise, such as variance in illumination, textureless objects, occlusion and surface reflectance which cause these descriptors to perform poorly. However, with the advent of RGB-D data we can combine the visual appearance and shape information in a fully descriptive and discriminative manner. Thus, in our approach we follow the standard VO workflow, with the novelty

of applying the feature detection and feature tracking components on both RGB and Depth images (i.e. we use both visual and shape keypoint extraction algorithms and a combined RGB-D feature detector) and the 6DOF rigid motion is estimated using the 3D points corresponding to the extracted feature points.

3.1.1. RGB-D Keypoint Extraction. In order to extract the most salient keypoints both on the RGB ($i_k \in I$ for $k = 1..N$) and Depth image ($d_k \in D$ for $k = 1..N$) we compute a set of keypoints $k_{rgb} \in K_{rgb}$ from i_k using the Center Surrounded Extrema keypoint detector introduced by [Agrawal et al. 2008] and implemented as the STAR detector in the Open Source Computer Vision (OpenCV) library [Bradski 2000] and another set of key points $k_d \in K_d$ from d_k using the NARF (Normal Aligned Radial Feature) interest point detector which is applied by converting the depth data into a range image. Even though the NARF and STAR detectors identify different types of keypoints, this does not rule out the fact that a certain pixel region might be salient both with shape and texture, thus these two algorithms can provide the same key points. We define the final set of keypoints ($k \in K$) for an RGB-D frame ($i_k + d_k$) is $K = K_{rgb} \cup K_d$, where \cup is the union of the two sets of keypoints. In our implementation, the union represents combining both sets and removing duplicate keypoints.

3.1.2. RGB-D Feature Matching. Recently, researchers have taken the task to correctly combine and fuse appearance and shape descriptions into a unique feature descriptor. The outcome has been the introduction of several feature vectors, namely the Convolution k-means, EMK-Spin + EMK-SIFT, BRAND, CSHOT, PFHRGB, MeshHOG, VOSCH. A comparative overview of all of these previously mentioned feature vectors is presented in [Ali et al. 2013]. We chose to use the novel BRAND (Binary Robust Appearance and Normals Descriptor) feature descriptor introduced by [Nascimento et al. 2012]. It combines intensity and shape information in a binary bit string using a binary operator within a patch centered at a keypoint and has demonstrated to outperform the CSHOT feature descriptor, which is one of the dominant RGB-D feature descriptor algorithms. For a consecutive pair of RGB-D images $(i_{k-1} + d_{k-1}) \rightarrow (i_k + d_k)$ we compute a set of BRAND feature descriptors F_{k-1} and F_k and apply a brute-force descriptor matcher with the Hamming norm and cross checking the correspondences, which results in a set of matches $m_i \in M_{k-1}^k$, where $i = 1..N$ and N is the total number of frame-to-frame matches.

3.1.3. Correspondences Outlier Rejection. The corresponding frame-to-frame matches M_{k-1}^k are still prone to wrong data associations, thus we further filter the matches using a RANSAC outlier rejection algorithm that finds the homography H between the set of corresponding keypoints that compose M_{k-1}^k , transforms the key points of the $(k-1)$ -th frame to the image plane of the k -th frame, computes the reproduction error between these sets of points and removes the correspondences which surpass a user defined reproduction threshold. The result is a set of minimal consistent corresponding matches MM_{k-1}^k between $(i_{k-1} + d_{k-1}) \rightarrow (i_k + d_k)$. Our acquired RGB-D images are already pre-calibrated, thus we can automatically compute MM_{k-1}^k in the cartesian space; i.e. 3D points $P_{k-1} \rightarrow P_k$, where $p \in P$ and $p = (x, y, z)$.

3.1.4. 6D Rigid Motion Estimation. Once the final corresponding matches MM_{k-1}^k are obtained, we compute the 6D rigid motion (inspired by RANSAC) by iteratively estimating the best transformation between the two sets of 3D points P_{k-1} and P_k , corresponding to the remaining correspondences. We set a maximum number of hypotheses iterations N where we randomly select s samples from MM_{k-1}^k . We extract the 3D points of the s corresponding matches and estimate a transformation hypothesis us-

ing the Umeyama Method [Umeyama 1991].³ This yields to a transformation matrix $T_i = [R_i, t_i]$, where $i = 1, \dots, N$. We then compute a transformation error e_i corresponding to T_i by computing the Root Mean Square (RMS) error based on the euclidean distances between the transformed set of points $P_{k-1}^t = T_i P_{k-1}$ and P_k . After computing N transformation hypotheses, the transformation T_i that produces the minimum error e_i is chosen as the final rigid motion transformation hypothesis. The resulting rigid transformation T_{k-1}^k aligns $P_{k-1} \rightarrow P_k$ and consequently camera poses $C_{k-1} \rightarrow C_k$. The complete iterative rigid motion estimation approach is provided in the online Appendix.

3.2. Camera Pose Fine Tuning and Surface Reconstruction with KinectFusion Large Scale

As mentioned earlier, KinectFusion is based on incrementally fusing consecutive frames of depth data into a 3D volumetric representation of an implicit surface. This representation is the truncated signed distance function (TSDF) [Curless and Levoy 1996]. The TSDF is basically a 3D point cloud stored in GPU memory using a 3D voxelized grid. The global TSDF is updated when a new depth image frame is acquired and the current camera pose is estimated. Initially, the depth image from the Kinect sensor is smoothed out using a bilateral filter [Yang 2012], which up-samples the raw data and fills the depth discontinuities. Then the camera pose of the current depth image frame is estimated with respect to the global model by applying a fast Iterative-Closest-Point (ICP) algorithm between the currently filtered depth image and a predicted surface model of the global TSDF extracted by ray casting. Once the camera pose is estimated, the current depth image is transformed into the coordinate system of the global TSDF and updated. Following we describe in detail the camera pose estimation method and the global TSDF update procedure.

3.2.1. Camera Pose Estimation. As mentioned earlier, we adapt the KinectFusion algorithm by initially transforming the new depth data with the coarse alignment estimated by 6D RGB-D odometry T_{rgbD} . Thus, we define the source points as $P_s = (T_{k-1}^k)^{-1} P_k$ and the target points P_t as the predicted surface model of the global TSDF. Then we apply ICP to fine-tune the transformation between P_s and P_t . The principal of the ICP algorithm is to find a data association between the subset of the source points (P_s) and the subset of the target points (P_t) [Besl and McKay 1992][Chen and Medioni 1991]. We use a special variant of the ICP-algorithm, the point-to-plane ICP [Zhang 1994]. It minimizes the error along the surface normal of the target points n_t , as in the following equation:

$$T^* = \underset{T}{\operatorname{argmin}} \sum_{p_s \in P_s} \|n_t \cdot (T(p_s) - p_t)\|_2 \quad (2)$$

where $n_t \cdot (T(p_s) - p_t)$ is the projection of $(T(p_s) - p_t)$ onto the sub-space spanned by the surface normal (n_t). Now, for every k -th frame of the recorded trajectory, the incremental rigid motion is estimated as $T_{k-1}^k = (T^*)^{-1}$. The resulting camera pose estimations of a freely moving handheld kinect recorded from the freiburg1_room and freiburg2_desk sequences can be seen in Fig. 2.

3.2.2. Global TSDF Updating. After computing transformation T^* , the new depth image is transformed into the coordinate system of the global TSDF by $T^*(P_s)$. The global model is represented in a voxelized 3D grid and integrated using a simple weighted running average. For each voxel, we have a value of signed distance for a specific voxel

³Derivation provided in our online Appendix.

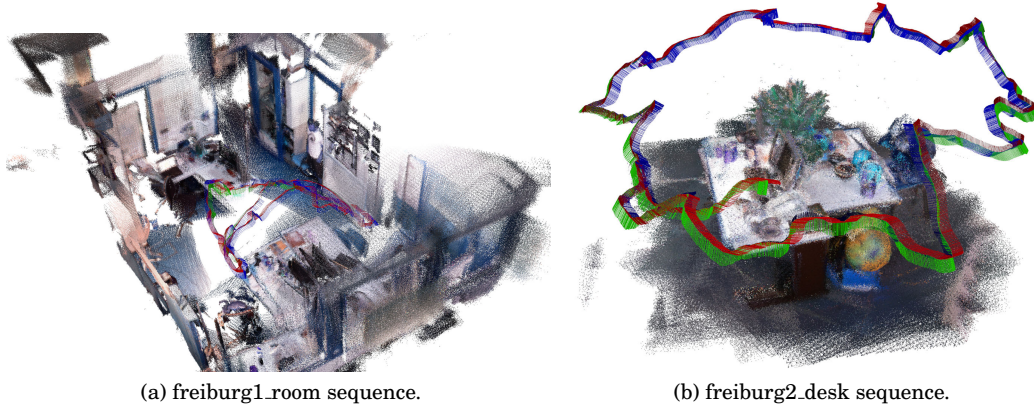


Fig. 2: Projected camera poses on a voxelized volumetric representation of the reconstructed map from the RGB-D Benchmark.

point x as $d_1(x), d_2(x), \dots, d_n(x)$ from n depth images ($d_i \in D$) in a short time interval. To fuse them, we define n weights $w_1(x), w_2(x), \dots, w_n(x)$. Thus, the weight corresponding point matching can be written in the form

$$w_n^* = \arg \sum_k^{n-1} \|W_k S_k - S_n\|_2 \quad (3)$$

where S_{k+1} is the cumulative TSDF and W_{k+1} is the weight functions after the integration of the current depth image frame, as described by [Curless and Levoy 1996]. Furthermore, by truncating the updated weights to a certain value W_α a moving average reconstruction is obtained.

3.2.3. World Model Update and Volume Shifting. In the original implementation of KinectFusion, the global TSDF is restricted to a fixed volume based on the resolution of the volumetric representation and the GPU memory capacity. In KinectFusion extension for large scale environments implemented by Heredia and Favier, where they allow the TSDF volume to move using a 3D cyclic buffer as the camera pose translation reaches a specified distance from the initial origin. Once the camera pose reaches this boundary, the origin of the TSDF volume is shifted and the slice of the 3D data that remains outside of the new volume is integrated to the world model.

3.3. Meshing with Marching Cubes

After obtaining the final world model, the polygon mesh is extracted by applying the marching cubes algorithm to the voxelized grid representation of the 3D reconstruction [Lorensen and Cline 1987]. The marching cubes algorithm extracts a polygon mesh by subdividing the points cloud or set of 3D points into small cubes (voxels) and marching through each of these cubes to set polygons that represent the isosurface of the points lying within the cube. This results in a smooth surface that approximates the isosurface of the voxelized grid representation, as can be seen in Fig. 3.

4. EXPERIMENTAL RESULTS

To validate the capabilities of our proposed algorithm, we conduct our evaluation on the RGB-D SLAM Dataset and Benchmark provided by [Sturm et al. 2012]. This

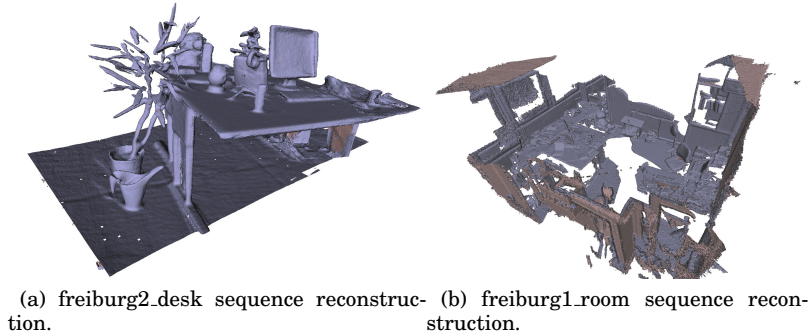


Fig. 3: Polygon mesh representation of the RGB-D Benchmark sequences after successfully applying our proposed approach.

dataset contains RGB-D data and ground-truth data targeted at the evaluation of visual odometry and visual SLAM systems. The data was recorded at the full frame rate of a Microsoft Kinect (30 Hz). The ground-truth trajectory was recorded from motion capture system with eight high-speed tracking cameras at 100 Hz. We chose to use two specific sequences of the *Handheld SLAM* category: (i) freiburg2_desk and (ii) freiburg1_room. The first sequence is a recording of a typical office scene with two desks, a computer monitor, keyboard, phone, chairs, etc. The second sequence is a recording of a trajectory through a whole office. In both sequences the Kinect is moved around the area and the loop is closed, so we can compare our results with the publicly available trajectories estimated by the RGB-D SLAM system presented by [Endres et al. 2012].

4.1. Performance

The proposed indoor mapping algorithm was tested on a laptop running Ubuntu 12.10 with an Intel Core i7-3720QM processor, 24GB of RAM and an NVIDIA™ GeForce™ GTX 670M with 3GB GDDR5 VRAM. With these specifications the original KinectFusion algorithm runs at ~ 10 fps, on the other hand the pure 6D RGB-D odometry method runs as ~ 5 fps, consequently the runtime of our combined proposed approach is ~ 3.3 fps. We have identified that the most time consuming processes of the 6D RGB-D odometry approach are the computation of the NARF keypoints on the range image, normal estimation of the depth images and multiple data conversions from PCL to OpenCV format for the BRAND feature computation. Even though our target is not real-time performance but accuracy and map consistency, by optimizing the implementation we predict that the algorithm can reach real-time performance. Furthermore, the current processing time per frame is equal to that of the RGB-D SLAM system proposed by [Endres et al. 2012].

4.2. Evaluation

As mentioned previously, we have evaluated our approach on the freiburg2_desk and freiburg1_room sequences. KinFu Large Scale³ performs properly in the freiburg2_desk sequence and yields to nearly the same accuracy as our approach. However, when applied on the freiburg1_room sequence, it fails to incrementally estimate the camera poses due to the planar surfaces of the walls and closets. This can be seen in Fig. 4. KinFu Large Scale performs quite well up until pose 530, which is when the dense ICP starts computing pose estimates with drift and finally fails in finding an estimate at around camera pose 540. We illustrate this same trajectory with our com-

bined approach. As can be seen, our 6D RGB-D odometry method in combination with KinFu Large Scale, shows no sign of drift and moreover alleviates the failure from using dense ICP based solely on the depth information.

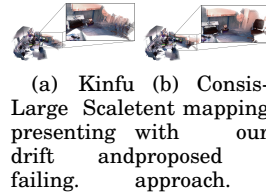


Fig. 4: Comparison of pose estimation methods on freiburg1_room sequence from pose 1-540. Zoomed in section are poses 530-540.

In order to provide a substantial numerical comparison, we evaluate the quality of the estimated camera trajectories on the dataset sequences using the automatic evaluation tool for RGB-D SLAM results, provided by the RGB-D benchmark. We compare the absolute trajectory error [m] and the relative pose error [m and $^{\circ}$] of the estimated camera trajectories with the ground truth data collected from a highly accurate motion capture system. In order to have a fair comparison between both methods, we compute the relative pose error for pose pairs with a distance of 1s between them. In Table I we present several error metrics (Std - standard deviation, Median, RMS - root mean square, Mean, Max - maximum) based on the absolute and relative trajectory errors. In the freiburg2_desk sequence our method shows comparable results with the RGB-D SLAM accuracy, we provide some minor improvements in the absolute trajectory error. This behavior was predicted, since this dataset has many salient visual as well as depth features, both algorithms perform well. Furthermore, the trajectory resembles more or less a circular loop with minimum change in elevation and rotation. These characteristics in a trajectory enable the pose graph optimization to be quite straight-forward, instead of distributing the error it is minimized appropriately.

Nonetheless, for more difficult scenes and trajectories (like the freiburg1_room sequence) our method not only improves the behavior of KinFu Large Scale but it also outperforms RGB-D SLAM. We provide a maximum relative pose translational error of 0.16m and rotational of 8.6° as opposed to 0.55m and 13.98° from RGB-D SLAM. Clearly, for extended spaces and rooms where there is a lack of descriptive surfaces, our approach gives the most consistent trajectories and maps, as can be seen in Fig.3. Let's recall that these results are after loop closure and graph optimization regarding the RGB-D SLAM approach. This means that graph pose optimization was not able to completely minimize the propagated errors from visual odometry, instead it distributed the errors throughout the trajectory. The differences between the estimated trajectories of each method and the ground truth can be found in the appendix.

5. CONCLUSION

In this work, we presented our first efforts into creating a consistent reconstruction of indoor spaces by augmenting the highly accurate KinectFusion with a novel 6D RGB-D odometry algorithm. We tested our combined approach on a notable RGB-D Benchmark dataset and present highly encouraging results. We provide nearly half of the absolute and relative pose errors from a state-of-the-art RGB-D SLAM system. An important contribution of this paper is that we demonstrate that the fusion of color and depth information yields to robust frame-to-frame alignment as opposed to solely

Sequence		freiburg2_desk		freiburg1_room	
		RGB-D SLAM	Our Approach	RGB-D SLAM	Our Approach
Absolute Trajectory Error [m]	Std	0.0160	0.0509	0.0706	0.0833
	Median	0.0946	0.0671	0.0487	0.1735
	RMS	0.0950	0.0949	0.1011	0.1972
	Mean	0.0936	0.0801	0.0723	0.1787
	Max	0.1458	0.2543	0.4365	0.4164
Relative Pose Error [m]	Std	0.0083	0.0171	0.0784	0.0308
	Median	0.0130	0.0145	0.0363	0.0461
	RMS	0.0167	0.0258	0.0953	0.0595
	Mean	0.0144	0.0194	0.0542	0.0509
	Max	0.0926	0.1208	0.5580	0.1615
Relative Pose Error [°]	Std	0.3294	0.7983	2.0767	1.3037
	Median	0.0089	0.0123	0.0337	0.0446
	RMS	0.6607	1.2329	3.1566	2.9982
	Mean	0.5727	0.9395	2.3772	2.6999
	Max	3.0105	6.1661	13.987	8.6952

Table I: Comparative results of absolute and relative trajectory errors against ground truth data.

using RGB (as in typical visual odometry approaches) or depth (as in the KinectFusion algorithm), which is the most important component of a 3D mapping application. Furthermore, the use of a consumer device such as the Microsoft Kinect opens up the possibility of open source personal 3D mapping, i.e. reconstructing your own environment with freely available software and sharing the reconstructed environments for many possible applications such as creating interactive virtual worlds.

REFERENCES

- Motilal Agrawal, Kurt Konolige, and Morten Rufus Blas. 2008. CenSurE: Center surround extremas for real-time feature detection and matching. In *Proceedings of the European Conference on Computer Vision*. 102–115.
- Haider Ali, Faisal Shafait, Eirini Giannakidou, Athena Vakali, Nadia Figueroa, Theodoros Varvadoukas, and Nikolaos Mavridis. 2013. Contextual object category recognition in RGB-D scene labeling. *To appear in Robotics and Autonomous Systems* (2013).
- Herbet Bay, Andreas Ess, Tinne Tuytelaars, and Luc van Gool. 2008. SURF: Speeded up robust features. *Computer Vision and Image Understanding* 110, 3 (2008), 346–359.
- Paul J. Besl and Neil D. McKay. 1992. A method for registration of 3D shapes. *IEEE Transactions on Pattern Analysis and Machine Intelligence* 14, 2 (1992), 239–256.
- Gary Bradski. 2000. The OpenCV library. *Dr. Dobb's Journal of Software Tools* (2000).
- Yang Chen and Gérard Medioni. 1991. Object modeling by registration of multiple range images. In *Proceedings of IEEE International Conference on Robotics and Automation*. 2724–2729.
- Brian Curless and Marc Levoy. 1996. A volumetric method for building complex models from range images. In *Proceedings of the 23rd Annual Conference on Computer Graphics and Interactive Techniques*. 303–312.
- Felix Endres, Jürgen Hess, Nikolas Engelhard, Jürgen Sturm, Daniel Cremers, and Wolfram Burgard. 2012. An evaluation of the RGB-D SLAM system. In *Proceedings of the IEEE International Conference on Robotics and Automation*. 1691–1696.
- Nadia Figueroa, Haider Ali, and Florian Schmidt. 2012. 3D registration for verification of humanoid Justin's upper body kinematics. In *Proceedings of the Ninth Conference on Computer and Robot Vision*. 276–283.
- William E. Lorensen and Harvey E. Cline. 1987. Marching cubes: A high resolution 3D surface construction algorithm. *Computer Graphics* 21, 4 (1987), 163–169.

- David G. Lowe. 2004. Distinctive image features from scale-invariant keypoints. *International Journal of Computer Vision* 60, 2 (2004), 91–110.
- Erickson R. Nascimento, Gabriel L. Oliveira, Mario F. M. Campos, Antônio W. Vieira, and Williamson Robson Schwartz. 2012. BRAND: A robust appearance and depth descriptor for RGB-D images. In *Proceedings of the IEEE/RSJ International Conference on Intelligent Robots and Systems*. 1720–1726.
- Richard A. Newcombe, Shahram Izadi, Otmar Hilliges, David Molyneaux, David Kim, Andrew J. Davison, Pushmeet Kohli, Jamie Shotton, Steve Hodges, and Andrew W. Fitzgibbon. 2011. KinectFusion: Real-time dense surface mapping and tracking. In *Proceedings of the 10th IEEE International Symposium on Mixed and Augmented Reality*. 127–136.
- Davide Scaramuzza and Friedrich Fraundorfer. 2011. Visual odometry [Tutorial]. *IEEE Robotics Automation Magazine* 18, 4 (2011), 80–92.
- Jürgen Sturm, Nikolas Engelhard, Felix Endres, Wolfram Burgard, and Daniel Cremers. 2012. A benchmark for the evaluation of RGB-D SLAM systems. In *Proceedings of the IEEE/RSJ International Conference on Intelligent Robots and Systems*. 573–580.
- Shinji Umeyama. 1991. Least-squares estimation of transformation parameters between two point patterns. *IEEE Transactions on Pattern Analysis and Machine Intelligence* 13, 4 (1991), 376–380.
- Thomas Whelan, Hordur Johannsson, Michael Kaess, John J. Leonard, and John McDonald. 2012. *Robust tracking for real-time dense RGB-D mapping with Kintinuous*. Technical Report MIT-CSAIL-TR-2012-031. Computer Science and Artificial Intelligence Laboratory, MIT.
- Qing Xiong Yang. 2012. Recursive bilateral filtering. In *Proceedings of the 12th European Conference on Computer Vision*. 399–413.
- Zhengyou Zhang. 1994. Iterative point matching for registration of free-form curves and surfaces. *International Journal of Computer Vision* 13, 2 (1994), 119–152.

Received December 16, 2013; revised ; accepted March 22, 2014

Online Appendix to: A Combined Approach Towards Consistent Reconstructions of Indoor Spaces based on 6D RGB-D Odometry and KinectFusion

Nadia Figueroa, Ecole Polytechnique Federale de Lausanne (EPFL)
Haiwei Dong, University of Ottawa
Abdulmotaleb El Saddik, University of Ottawa and New York University AD

A. UMEYAMA RIGID MOTION DERIVATION

This method demeans the 3D point sets as

$$\begin{aligned} p'_{k-1,i} &= p_{k-1,i} - \bar{p}_{k-1} \\ p'_{k,i} &= p_{k,i} - \bar{p}_k \\ \forall_i : p'_{k,i} &= R p'_{k-1,i} \\ P'_{k-1} &= R P'_{k-1} \end{aligned} \quad (4)$$

and computes the rotational component with the Singular Value Decomposition of the correlation matrix and the translation component based on the mean positions as follows

$$\begin{aligned} svd(P'_{k-1}, P'_k)^T &= UDV^T \\ R &= VU^T \\ t &= \bar{p}_{k-1} - R\bar{p}_k. \end{aligned} \quad (5)$$

B. RIGID MOTION ESTIMATION ALGORITHM

ALGORITHM 1: Iterative Rigid Motion Estimation

Input: Corresponding matches MM_{k-1}^k , source point cloud P_{k-1} , target point cloud P_k , maximum number of hypotheses iterations N , number sample correspondences s and error threshold e_t

Output: A rigid transformation $T_{k-1,rgb}^k$ that aligns $P_{k-1} \rightarrow P_k$

for i in N **do**

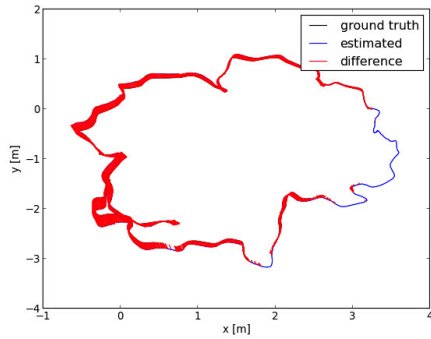
$mm_i \leftarrow findRandomCombinations(MM_{k-1}^k, s)$
 $T_i \leftarrow computeUmeyamaRigidMotion(P_{k-1}, P_k, mm_i)$
 $e_i \leftarrow computeTransformationError(P_{k-1}, P_k T_i)$

end for

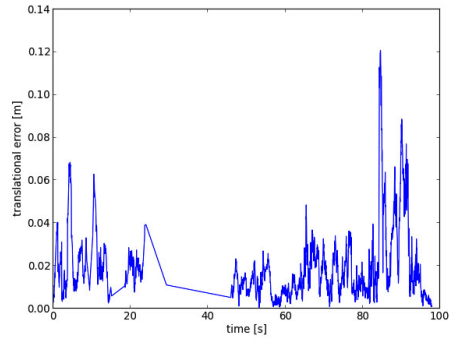
$T_{k-1,rgb}^k \leftarrow findMinimumTransformationError(e_i \in e \text{ and } T_i \in T \text{ for } i = 1..N)$

C. EVALUATION

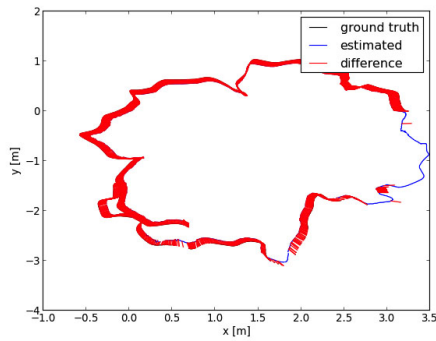
For each sequence we provide two plots: (i) the trajectory difference and (ii) the relative translational error. These trajectory differences represent the pose pair errors between the estimated and ground truth trajectories and is illustrated with a red vector connecting the pose pairs.



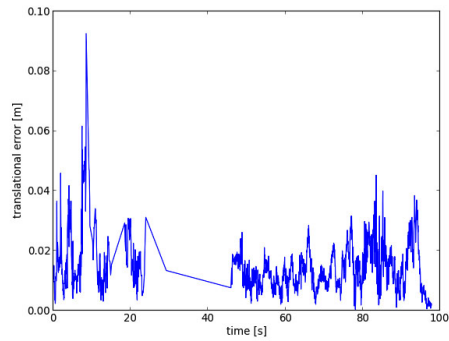
(a) Trajectory difference with our approach.



(b) Translational errors of our approach.

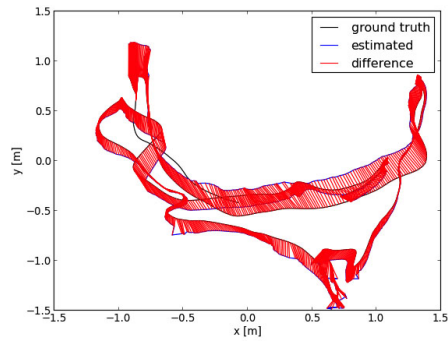


(c) Trajectory difference with RGB-D SLAM.

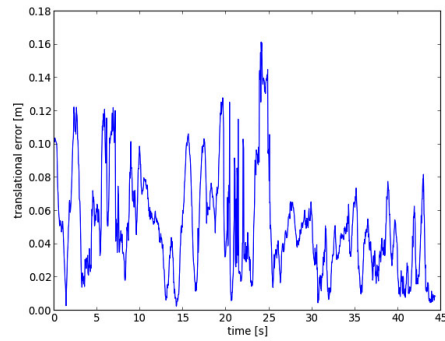


(d) Translational errors of RGB-D SLAM.

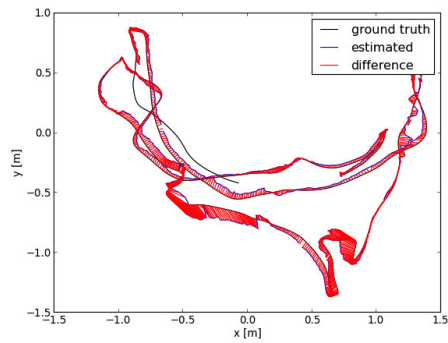
Fig. 5: Estimated trajectories (a,c) of the freiburg2.desk sequence compared to the ground truth and relative translational errors (b,d) for RGB-D SLAM (top row) and our approach (bottom row).



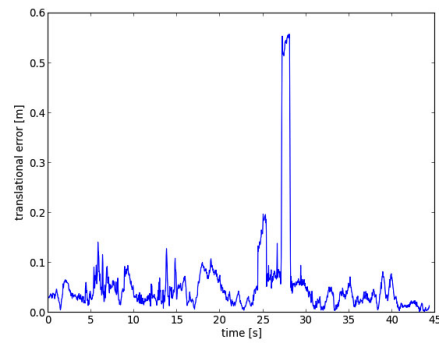
(a) Trajectory difference with our approach.



(b) Translational errors of our approach.



(c) Trajectory difference with RGB-D SLAM.



(d) Translational errors of RGB-D SLAM.

Fig. 6: Estimated trajectories of the freiburg1_room sequence compared to the ground truth and relative translational errors (b,d) for RGB-D SLAM (top row) and our approach (bottom row).